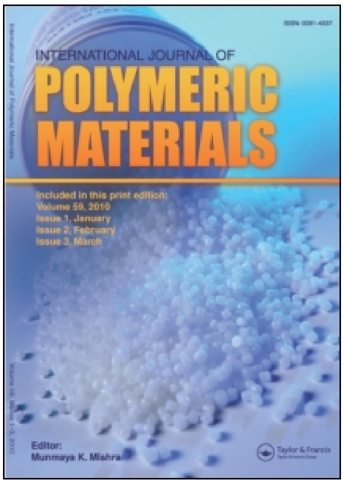

International Journal of Polymeric Materials
Publication details, including instructions for authors and subscription information:
http://www.informaworld.com/smpp/title~content=t713647664

Nonisothermal Curing Kinetics and Physical Properties of Unsaturated Polyester Modified with EA-POSS

Jungang Gao[a]; Cuifang Dong[a]; Yonggang Du[a]
[a] College of Chemistry and Environmental Science, Hebei University, Baoding, China

To cite this Article Gao, Jungang , Dong, Cuifang and Du, Yonggang(2010) 'Nonisothermal Curing Kinetics and Physical Properties of Unsaturated Polyester Modified with EA-POSS', International Journal of Polymeric Materials, 59: 1, 1 — 14
To link to this Article: DOI: 10.1080/00914030903172866
URL: http://dx.doi.org/10.1080/00914030903172866

International Journal of Polymeric Materials, 59:1–14, 2010
Copyright © Taylor & Francis Group, LLC
ISSN: 0091-4037 print/1563-535X online
DOI: 10.1080/00914030903172866

Nonisothermal Curing Kinetics and Physical Properties of Unsaturated Polyester Modified with EA-POSS

Jungang Gao, Cuifang Dong, and Yonggang Du

College of Chemistry and Environmental Science, Hebei University, Baoding, China

The polyhedral oligomeric silsesquioxanes (EA-POSS) which contain epoxy acrylate group were synthesized from 3-glycidypropyl-trimethoxysilane (GTMS) and acrylic acid in two steps: hydrolytic condensation of GTMS and esterification of polyhedral oligomeric silsesquioxanes epoxy resin (POSSER) with acrylic acid under appropriate conditions. The unsaturated polyester resin (UPR) was mixed with EA-POSS at different proportions, and the cure kinetics were investigated by nonisothermal differential scanning calorimetry (DSC) technique. The results show that UPR, the methyl methacrylate and EA-POSS have very good compatibility and can co-cure in free radical polymerization. The curing reaction can be described by a two-parameter autocatalytic Šesták-Berggren (S-B) model and kinetic equations are obtained. The reaction rate is increased with the addition of EA-POSS. The electrical properties of fiberglass-reinforced laminates, thermal stability and dynamic mechanical properties of EA-POSS/UPR nanocomposites were determined. The results indicate that these properties are all modified after EA-POSS is added to the UPR. The mechanical loss peak temperature T_p increases by about 30–35°C and the initial decomposition temperature increases by about 15°C.

Keywords cure kinetics, electrical properties, silsesquioxanes, thermal stability, unsaturated polyester resins

---

Received 11 May 2009; in final form 15 June 2009.

The authors gratefully acknowledge the financial support from the Nature Science Foundation (No. E2007000204) of Hebei Province, China.

Address correspondence to Jungang Gao, College of Chemistry and Environmental Science, Hebei University, Baoding 071002, People's Republic of China. E-mail: gaojg@mail.hbu.edu.cn

INTRODUCTION

Organic-inorganic hybrid nanocomposite materials have attracted a great deal of attention because of their potential applications in optics, electronics, engineering and bioscience. Organic-inorganic hybrid polymeric materials with an in situ created inorganic phase are typical nanocomposite materials, which have received significant interest in recent years [1,2]. Nanostructured hybrid organic-inorganic composites typically exhibit mechanical properties superior to the parent materials. Many polymers, including polyimide, epoxy, polystyrene, poly (dimethyl siloxane), and others have been used to produce hybrid materials [3–5].

Polyhedral oligomeric silsesquioxane (POSS) is a new type of organic-inorganic hybrid molecule whose structure short-form is $(RSiO_{1.5})_n$. POSS structure is shown in Scheme 1. It has a Si-O nanostructured inorganic framework as the core and reactive or nonreactive functional groups around the inorganic framework. The reactive functional groups on POSS not only can further homopolymerize, but also can react or copolymerize with other reactants or monomers. The introduction of nonreactive functional groups into POSS can change the solubility and compatibility between POSS and polymers [6–9].

Unsaturated polyester resin (UPR) is one of the most important thermosetting polymers. It has relatively low cost, good balance of properties, and adaptability to many fabrication processes, so it has been widely used as the matrix resin for polymeric composites. The unsaturated polyester is normally prepared by the reaction of a saturated diol with a mixture of an unsaturated dibasic acid and a saturated dibasic acid or its corresponding anhydride. The

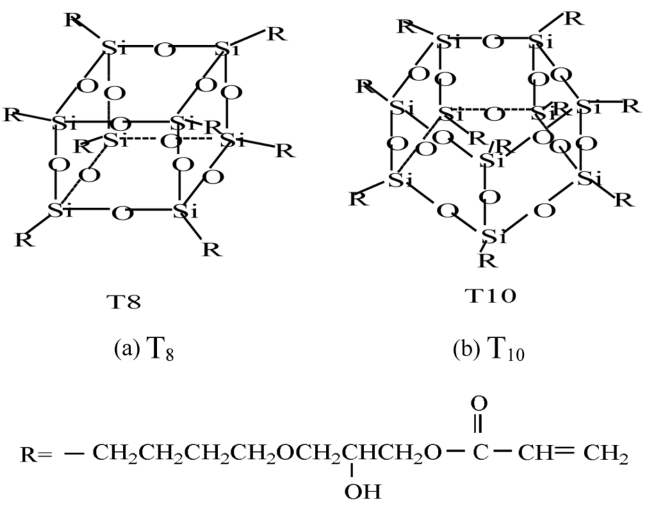

(a) T_8 (b) T_{10}

$$R= -CH_2CH_2CH_2CH_2OCH_2\underset{OH}{CH}CH_2O-\overset{O}{\overset{\|}{C}}-CH=CH_2$$

Scheme 1: Molecular structure of EA-POSS T_8 and T_{10}.

curing reaction of unsaturated polyester is a free radical chain growth polymerization. Before the reaction, the system contains styrene or methyl methacrylate monomers, unsaturated polyester molecules, initiators and curing agents. When the reaction starts, the initiator decomposes, forming free radicals to trigger the polymerization. Free radicals link adjacent unsaturated polyester units and form primary polymer chains through connecting styrene or methyl methacrylate monomers by both inter- and intramolecular reaction. The processing of thermosetting resin requires understanding of the rheology and the polymerization reaction kinetics during cure. The cure kinetics of unsaturated polyester is of considerable importance for the optimization of the manufacturing process [9].

In this article, in order to improve the properties of UPR, the POSS which contains polymerizable epoxy acrylate groups (EA-POSS) was added into the reaction system. The nonisothermal curing reaction of EA-POSS/UPR was investigated by differential scanning calorimeter (DSC), and the thermal stability, mechanical and electrical properties were determined.

EXPERIMENTAL

Materials

Methyl methacrylate (MMA), maleic anhydride, diethylene glycol, acrylic acid, benzoyl peroxide (BPO), N,N-dimethyl-benzylamine (DMBA), hydroquinone, toluol and isopropyl alcohol (IPA) are all analytically pure grade and were supplied by Tianjin Chem. Co., Tianjin, China; phthalic anhydride, analytically pure grade, was supplied by Beijing Reagent Co., Beijing, China; UPR was synthesized from maleic anhydride, phthalic anhydride, and diethylene glycol in accordance with the literature [10]. The acid value is $60 \sim 70$ mgKOH/g; 3-glycidypropyl-trimethoxysilane (GTMS) was supplied by Shenda Chem. Co., Beijing, China.

EA-POSS was synthesized in two steps: In the first step, the polyhedral oligomeric silsesquioxanes epoxy resin (E-POSS) was prepared from 3-glycidypropyl-trimethoxysilane (GTMS) and tetramethylammonium hydroxide (TMAH) by hydrolytic condensation according to the literature [11,12]. The yield is above 85 wt%. Liquid chromatography-mass spectrometer (LC/MS, 1100, Agilent Co., USA) was used for the determination of the components and the detailed structure of E-POSS. The result shows that T_{10} is the main product of the E-POSS synthesized by the above method, mixed with a little $T_{8.}$ In the second step, the quantitative solvent, catalyst (DMBA), inhibitor (hydroquinone) and stoichiometric acrylic acid were added to the above system and esterfied at 100–110°C for 4–6 h. Then the solvent and other small molecules were removed and EA-POSS was obtained [13]. The molecular structure of EA-POSS is shown in Scheme 1.

Apparatus and Equipment

Differential scanning calorimeter (DSC, Diamond type), thermogravimetric analyzer (TGA, pyris 6-type) and dynamic mechanical analyzer (DMA, 8000-type) were all made by Perkin Elmer Co., USA. High Resister (ZC36-type) was made by Precision Scientific Instrument Co., Shanghai, China; electric tensile tester (WSM-20KN) was made by Intelligent Equipment Co., Changchun, China.

Sample Preparation and Measurements

The five samples were prepared according to mass per cent of EA-POSS in total mixtures of EA-POSS, MMA, BPO and UPR, which is 0%, 5%, 10%, 15%, and 20% (marked as: No. 0, No. 5, No. 10, No. 15, No. 20), respectively. The ratio of MMA in total resin mixtures is 25%, the ratio of BPO is 0.5% of reaction mixture. Then all components were fully mixed at room temperature. About 8 mg of the sample was placed in a sealed aluminum sample pan. Curing reaction was carried out on DSC. The DSC instrument was calibrated with high-purity indium. Dynamic scans were conducted from 40 to 180°C under $20\,\mathrm{mL\,min^{-1}}$ nitrogen flow rate. The heating rate β is 3, 5, 7, 9, 11°C/min, respectively.

Determination of Physical and Mechanical Properties

The glass fiber cloth was boiled in Na_2CO_3 solution for 30 min and dried at 80°C. The fiberglass-reinforced laminates were made in 3 mm thickness, in which the content of EA-POSS/UPR resin was 40%. The laminates were heated and cured at 60, 80, 100 and 120°C respectively for 3 h. After being cooled to room temperature, the physical and mechanical properties were the determined.

RESULTS AND DISCUSSIONS

Co-curing Behavior

The co-curing behavior of all five samples was determined by the non-isothermal DSC method. The heating rate was 3, 5, 7, 9 and 11°C/min, respectively. Figure 1 shows the typical DSC thermograms of No. 5 and No. 10 samples recorded at the different heating rates. These thermograms provide information for determining the condition of co-curing reactions. As seen from Figure 1, the initial curing temperature (T_{ci}), the peak temperature (T_{cp}) and the finishing temperature (T_{cf}) all increase with the heating rate, but the curing duration time decreases. This is because at the increasing heating rate,

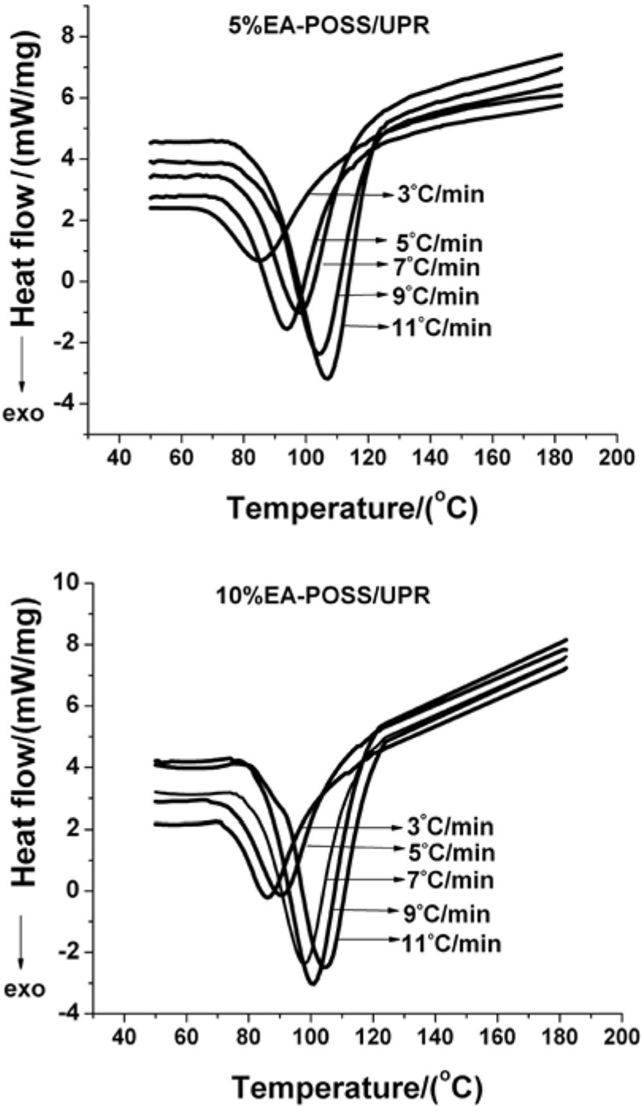

Figure 1: Nonisothermal DSC curves of EA-POSS/UPR systems at different heating rates.

dH/dt increases, the thermal effect in the unit time increases and the temperature difference also increases. Therefore, the exothermic peak of the co-curing reaction move to the high temperature and the curing reaction is accelerated.

Also, every DSC curve of the EA-POSS/UPR system is very smooth and only has one evident co-curing peak at the selected heating rates. This result illuminates that the compatibility of this system is good and co-curing can form homogeneous nanocomposites. The other three samples show similar

Table 1: Static curing temperature parameters of EA-POSS/UPR systems.

	***wt*% (EA-POSS)%**				
Temperature (°C)	**0**	**5**	**10**	**15**	**20**
T_{ci}	67.419	68.792	66.907	69.901	69.680
T_{cp}	85.912	78.982	79.165	80.501	81.274
T_{cf}	91.806	87.311	88.330	89.821	89.862

results under the same co-curing conditions. From plots of (T_{ci}), (T_{cp}) and (T_{cf}) vs. heating rates β the reaction temperatures at static condition can be obtained and are shown in Table 1.

Isoconversional Activation Energy

The basic assumption for the application of DSC technology to the curing reaction of thermosets is that the reaction rate of the kinetic process ($d\alpha/dt$) is proportional to the measured heat flow (dH/dt) [14,15].

$$\frac{d\alpha}{dt} = \frac{dH}{dt} \cdot \frac{1}{\Delta H} \tag{1}$$

where ΔH is the enthalpy of the curing reaction, α is the extent of reaction or conversion, $d\alpha/dt$ is the reaction rate of the kinetic process, dH/dt is the measured heat flow.

The reaction rate of the kinetic process can be described by Eq. (2)

$$\frac{d\alpha}{dt} = k(T)f(\alpha) \tag{2}$$

where $f(\alpha)$ is the dependent kinetic model function, $k(T)$ is the temperature-dependent reaction rate constant and follows an Arrhenius form:

$$k(T) = A\exp\left(\frac{-E_a}{RT}\right) \tag{3}$$

where A is the pre-exponential factor and E_a is the apparent activation energy. Thus the kinetic equation can be described by Eq. (4)

$$\frac{d\alpha}{dt} = A\exp\left(\frac{-E_a}{RT}\right)f(\alpha) \tag{4}$$

For non-isothermal curing process, the Kissinger isoconversional method can be applied to different degrees of conversion α. Equation (5) is known as Kissinger equation [16,17]:

$$\ln\left(\frac{\beta}{T^2}\right) = \ln\left(\frac{AR}{E_a}\right) - \frac{E_a}{RT} \tag{5}$$

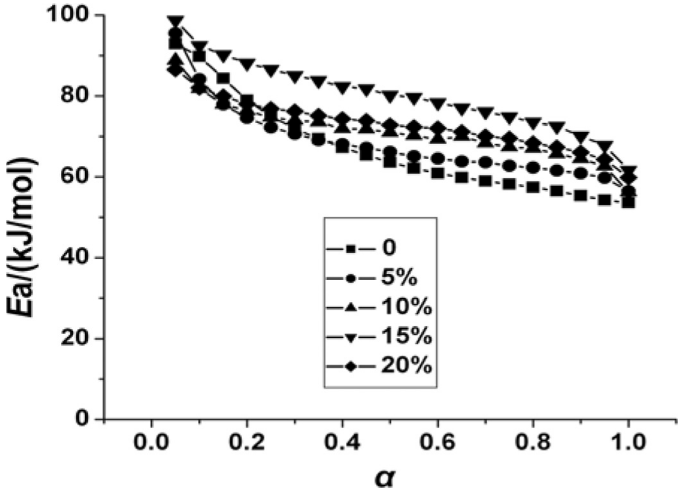

Figure 2: Relationships of E_a vs. α for EA-POSS/UPR systems.

The slope of $\ln(\beta/T^2)$ vs. $1/T$ gives values of $(-E_a/R)$, so the values of E_a at different conversions can be obtained.

Figure 2 shows the relationship of E_a vs. α for EA-POSS/UPR system. As seen from Figure 2, the values of E_a in the initial stage are higher than those of any other time for all samples; E_a tends to decrease slightly with the reaction progress. The E_a has only slight variation as conversion α between 0.2 and 0.9. This result is associated with the reaction mechanism. It shows that the initiator decomposition and triggering of the polymerization have a higher E_a. After that, a stable period of reaction ensures and a little change in E_a. But the E_a decrease again at the final stage. This is because that the system gels and diffusion control has exceeded the chemical kinetics control [18]. For example, the E_a of 5% EA-POSS/UPR sample has a little variation for conversion in the interval of $0.25 \leq \alpha \leq 0.9$, which is between 60–70 kJ/mol and the average value is 64.58 kJ/mol. The E_a of 10% EA-POSS/UPR sample has a little variation when the conversion is between 0.2 and 0.8, and the average E_a is 71.19 kJ/mol. The average E_a increases for the samples from No. 0 to No. 15, which is related with crosslink degree, because the crosslink degree and viscosity of reaction system will increase with increasing content of EA-POSS. But the lower average E_a for No. 20 than that of No. 15 may be related to diffusion control effect at a higher crosslink degree.

Curing Reaction Kinetics

If the value of $f(\alpha)$ is assumed to be the same at different heating rates when the value of α is the same, then the values of E_a can be used to find the appropriate kinetic model which can best describe the conversion function of the curing process [19,20]. The most suitable kinetic model can be evaluated with the functions of $y(\alpha)$ and $z(\alpha)$ according to the Eqs. (6) and (7):

$$y(\alpha) = \frac{d\alpha}{dt} e^{u} \tag{6}$$

$$z(\alpha) = N(u)\frac{d\alpha}{dt} T \tag{7}$$

where u is reduced activation energy E_a/RT, $N(u)$ is the expression of the temperature integral, which can be well approximated using the fourth rational expression as in Eq. (8):

$$N(u) = \frac{u^3 + 18u^2 + 88u + 96}{u^4 + 20u^3 + 120u^2 + 240u + 120} \tag{8}$$

The $y(\alpha)$ function is proportional to $f(\alpha)$ function, being characteristic for a given kinetic model. The shape and the maximum of both $y(\alpha)$ and $z(\alpha)$ functions, give valuable information for determination of the most suitable kinetic model.

So, in our present research, the average value of E_a was used to calculate both the $y(\alpha)$ and $z(\alpha)$ functions with Eqs. (6) and (7), respectively. Figures 3 and 4 describe the variation of the $y(\alpha)$ and $z(\alpha)$ functions with the α for sample No. 10 at different heating rates. The values of both the $y(\alpha)$ and $z(\alpha)$ are normalized within the (0,1). The α_M and α_P^∞ are the value of α while $y(\alpha)$ or $z(\alpha)$ gets the maximum value, respectively. α_P is the α maximum value of DSC peak. These parameters can help to decide the choice of the kinetic model. The

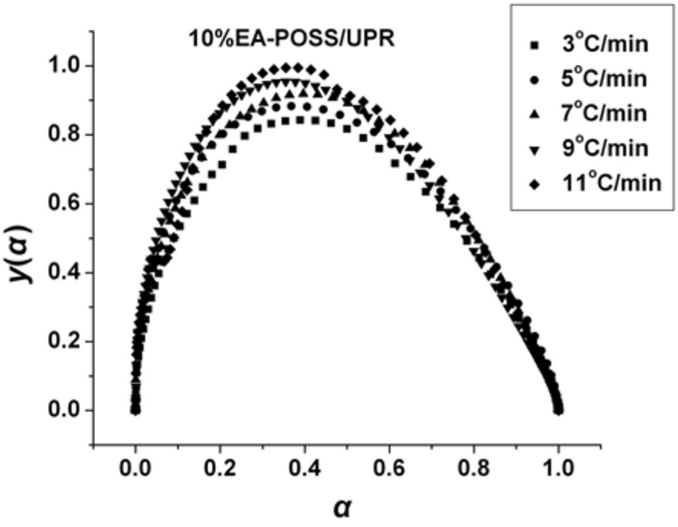

Figure 3: Variation of $y(\alpha)$ function versus α.

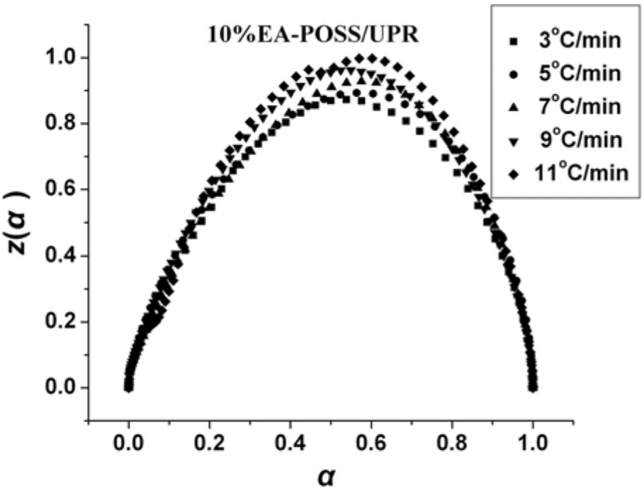

Figure 4: Variation of $z(\alpha)$ function versus α.

values of α_{M}, $\alpha_{\mathrm{P}}^{\infty}$ and α_{P} at different heating rates are shown in Table 2. As seen from Table 2, the values of α_{M}, $\alpha_{\mathrm{P}}^{\infty}$ and α_{P} are independent of the heating rate. Simultaneously, the values of α_{M} are lower than the values of α_{P}, while $\alpha_{\mathrm{P}}^{\infty}$ exhibits values lower than 0.632 (except No. 0). In accordance with the results of Málek on the cure kinetics under non-isothermal conditions [20], the studied curing process can be described using the two-parameter autocatalytic Šesták-Berggren (S-B) kinetic model [9,21,22].

$$f(\alpha) = \alpha^m (1-\alpha)^n \tag{9}$$

where m and n are the kinetic exponents. According Eq. (4), we have:

$$\frac{\mathrm{d}\alpha}{\mathrm{d}t} = A\exp\left(\frac{-E_{\mathrm{a}}}{RT}\right)\alpha^m(1-\alpha)^n \tag{10}$$

The kinetic parameter n is obtained by the slope of the linear dependence $\ln[(\mathrm{d}\alpha/\mathrm{d}t)e^u]$ vs. $\ln[\alpha^P(1-\alpha)]$, and $m = pn$, where $p = \alpha_M/(1-\alpha_M)$. Table 3 lists some kinetic parameters evaluated from the proposed Šesták-Berggren kinetic model. As seen from Table 3, the kinetic parameters of A, n, m are all increase when EA-POSS is added into the UPR, and has a higher reaction rate than pure UPR. This is because the acryl groups on POSS are all in the outside of EA-POSS and have a higher reaction probability.

From Eq. (10) and kinetic parameters of Table 3, we can obtain the curing kinetic equations of the studied systems as following:

$$\text{No. 0} \qquad \frac{\mathrm{d}\alpha}{\mathrm{d}t} = 1.24\times 10^{11}\exp\left(-\frac{66890}{RT}\right)\alpha^{0.393}(1-\alpha)^{0.688}$$

Table 2: The value of $\alpha_P{'}\alpha_M$ and α_P^{∞} at different heating rates.

wt% (EA-POSS)%	**β (°C/min)**	α_P	α_M	α_P^{∞}
0	3	0.6549	0.4735	0.6516
	5	0.7133	0.4405	0.7040
	7	0.7129	0.4544	0.7129
	9	0.6790	0.3454	0.6929
	11	0.6995	0.2298	0.7155
5	3	0.5183	0.3806	0.5409
	5	0.5661	0.4061	0.5771
	7	0.5652	0.3850	0.5790
	9	0.5678	0.4006	0.5843
	11	0.6022	0.3926	0.6118
10	3	0.5265	0.3923	0.5380
	5	0.5580	0.3783	0.5696
	7	0.5681	0.3964	0.5755
	9	0.5328	0.3620	0.5412
	11	0.5808	0.3646	0.5914
15	3	0.5161	0.3796	0.5205
	5	0.5265	0.3713	0.5450
	7	0.5209	0.3645	0.5363
	9	0.5021	0.3376	0.5211
	11	0.4919	0.3120	0.5029
20	3	0.5286	0.3849	0.5286
	5	0.5610	0.4269	0.5740
	7	0.5264	0.3827	0.5346
	9	0.5390	0.3677	0.5488
	11	0.5160	0.3697	0.5275

$$\text{No. 5} \qquad \frac{d\alpha}{dt} = 3.04 \times 10^{11} \exp\left(-\frac{64580}{RT}\right)\alpha^{0.453}(1-\alpha)^{0.701}$$

$$\text{No. 10} \qquad \frac{d\alpha}{dt} = 1.36 \times 10^{12} \exp\left(-\frac{71190}{RT}\right)\alpha^{0.444}(1-\alpha)^{0.729}$$

$$\text{No. 15} \qquad \frac{d\alpha}{dt} = 4.14 \times 10^{13} \exp\left(-\frac{81770}{RT}\right)\alpha^{0.449}(1-\alpha)^{0.831}$$

$$\text{No. 20} \qquad \frac{d\alpha}{dt} = 2.67 \times 10^{12} \exp\left(-\frac{73900}{RT}\right)\alpha^{0.457}(1-\alpha)^{0.728}$$

In order to verify the correctness of the kinetic model proposed with the S-B equation, we calculated the values of $d\alpha/dt$ using the data listed in Table 3 and simulated the curves of $d\alpha/dt$ vs. T. Figure 5 is the comparison of experimental and theoretical values for the 10% EA-POSS/UPR sample. As can be seen from Figure 5, the theoretical curves all match well with the experimental curves, but have a slight deviation at peak at the higher heating

Table 3: Curing kinetic parameters of EA-POSS/UPR systems.

wt% (EA-POSS)%	β (°C/min)	E_a (kJ/mol)	ln*A*	*m*	*n*
0	3	66.89	25.835	0.487	0.541
	5		25.582	0.405	0.514
	7		25.281	0.323	0.387
	9		25.374	0.355	0.672
	11		25.666	0.396	1.326
	Mean		25.548	0.393	0.688
5	3	64.58	26.747	0.494	0.805
	5		26.519	0.482	0.705
	7		26.590	0.486	0.776
	9		26.139	0.404	0.605
	11		26.202	0.397	0.614
	Mean		26.439	0.453	0.701
10	3	71.19	28.004	0.479	0.742
	5		28.216	0.466	0.766
	7		27.798	0.409	0.622
	9		28.008	0.475	0.836
	11		27.670	0.389	0.678
	Mean		27.939	0.444	0.729
15	3	81.77	31.601	0.497	0.813
	5		31.300	0.422	0.714
	7		31.163	0.389	0.678
	9		31.451	0.488	0.957
	11		31.262	0.450	0.991
	Mean		31.355	0.449	0.831
20	3	73.90	28.778	0.471	0.753
	5		28.678	0.474	0.636
	7		28.490	0.444	0.717
	9		28.599	0.439	0.755
	11		28.519	0.457	0.780
	Mean		28.613	0.457	0.728

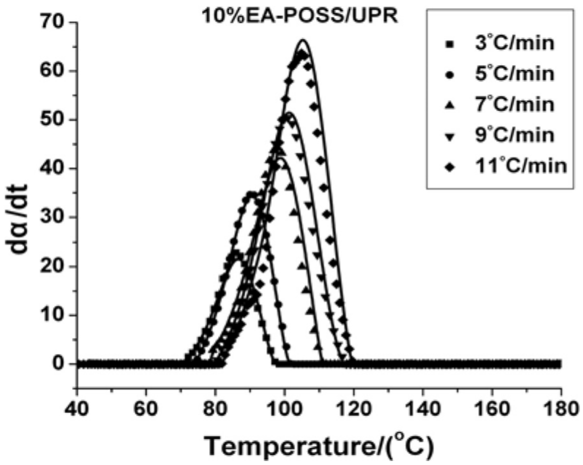

Figure 5: Comparison of experimental (dots) and calculated (full lines) DSC curves for 10% EA-POSS/UPR system.

Table 4: Electrical properties of EA-POSS/UPR systems.

wt% (EA-POSS)%	Rv (MΩ)	Rs (MΩ)	tan δ	ε
0	1.06×10^4	1.79×10^4	0.03734	1.174
5	1.64×10^4	3.67×10^4	0.02840	1.107
10	3.30×10^4	2.20×10^4	0.02558	1.075
15	1.93×10^4	1.42×10^4	0.02487	1.089
20	1.70×10^4	1.49×10^4	0.02628	1.093

rates. So, the two-parameter S-B model can be used to study the cure kinetics of EA-POSS/UPR systems.

Electrical Properties of Laminates

The electrical properties of fiberglass-reinforced laminates for EA-POSS/UPR systems were determined and are shown in Table 4. As seen from Table 4, the volume resistance Rv and surface resistance Rs of UPR laminates modified using EA-POSS all increase when EA-POSS content is not over 10%. But they decrease when EA-POSS content is over 10%, and the Rv is higher than pure UPR laminates until 20% EA-POSS content. The dielectric loss tan δ and dielectric constant ε are all decreased. These results show that some EA-POSS can improve the electric properties of UPR laminates.

Thermal Stability and Dynamic Mechanical Property

Table 5 shows the TGA data of cured EA-POSS/UPR. As seen from Table 5, initial decomposition temperature T_{di}, temperature of weight loss percentage 50% $\mathrm{T}_{\mathrm{d50}}$ and final residual percentage are all increased with the increasing content of the EA-POSS. The result shows that the composite of EA-POSS/UPR has a better thermal stability than pure UPR, that is, the EA-POSS can improve thermal stability of UPR.

Figure 6 is the DMA spectra of EA-POSS/UPR samples for different content (wt%) of EA-POSS. As seen from Figure 6, the mechanical loss peak temperatures T_{p} increase with increasing content of EA-POSS. This result shows that the EA-POSS not only can increase the thermal stability, but also

Table 5: TGA data of EA-POSS/UPR systems.

wt% (EA-POSS)%	T_{di} (°C)	T_{d50} (°C)	Residual (%)
0	215.5	372.8	0
5	226.8	382.8	2.390
10	224.8	387.5	3.363
15	228.6	391.6	4.282
20	231.2	397.4	5.581

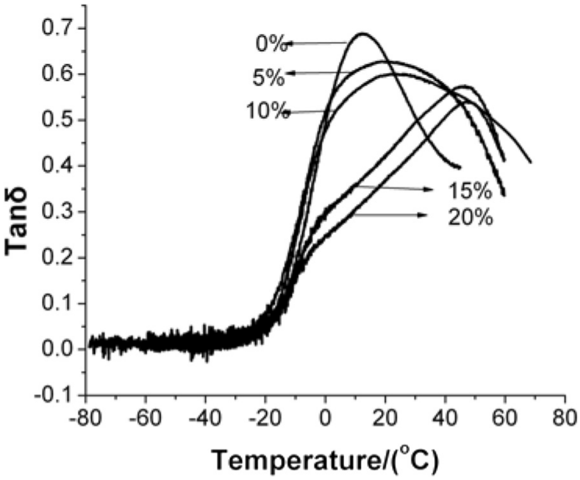

Figure 6: Dynamic mechanical spectra of EA-POSS/UPR systems.

increase thermal resistance or glass transition temperature T_g. This is because the crosslinking degree increases with increasing content of EA-POSS.

CONCLUSIONS

1. The polyhedral oligomeric silsesquioxanes, containing epoxy acrylate (EA-POSS), unsaturated polyester resin and MMA have together good compatibility. The non-isothermal curing reactions of EA-POSS/UPR samples at different heating rates all have a single smooth exothermic curing peak and can co-cure in free radical polymerization.
2. The non-isothermal curing reactions of EA-POSS/UPR can be described by a two-parameter autocatalytic Šesták-Berggren (S-B) model. The reaction rate is increased when EA-POSS is added, and the kinetic equations of curing reaction are obtained.
3. The electrical properties of fiberglass-reinforced laminate (FRP) are improved when EA-POSS is added, and the thermal stability and glass transition temperature T_g are also increased. When the content of EA-POSS is 15–20%, the mechanical loss peak temperature T_p can increase by about 30–35°C, the initial decomposition temperature can increase by 15°C.

REFERENCES

[1] Laurence, B., Jocelyne, M., and Florence, B. *Chem. Mater.* **7**, 975 (1995).
[2] Wen, J., and Wilkes, G. L. *Chem. Mater.*, **8**, 1667 (1996).

[3] Hajji, P., David, L., Gerard, J. F., Pascault, J. P., and Vigier, G. *J. Polym. Sci. Part B: Polym. Phys.* **37**, 3172 (1999).

[4] Iami, Y., Itoh, H., Naka, K., and Chujo, Y. *Macromolecules*, **33**, 1443 (2000).

[5] Tsumura, M., and Iwahara, T. *J. Appl. Polym. Sci.*, **78**, 724 (2000).

[6] Dell'Erba, I. E., and Williams, R. J. J. *Eur. Polym. J.* **43**, 2759 (2007).

[7] Kopesky, E. T., Mckinley, G. H., and Cohen, R. E. *Polymers*, **47**, 299 (2006).

[8] Gao, J., Kong, D., and Li, S. *Inter. J. Polym. Mater.* **57**, 940 (2008).

[9] Vilas, J. L., Laza, J. M., Garay, M. T., Rodriguez, M., and Leon, L. M. *J. Appl. Polym. Sci.*, **79**, 447 (2001).

[10] Braun, D., Cherdon, H., and Kern, W. (1972). *Techniques of Polymer Syntheses and Characterization [M]*, John Wiley, Huang, B. T. Translation, Sci Pub Co, China, 1981:245–247.

[11] Gao, J. G., Jiang, C. J., and Zhang, X. J. *Inter. J. Polym. Mater.* **56**, 65 (2007).

[12] Saito, H., and Isozaki, M. Japan, [31] **285387**[P], (2002).

[13] Gao, J. G., Dong, S. L., Dong, X. H., and Jiang, C. J. *China Adhesives*, **10**, 1 (2007).

[14] Jubsilp, C., Damrongsakkul, S., Takeichi, T., and Rimdusit, S. *Thermochimica Acta*, **447**, 131 (2006).

[15] Xu, G., Shi, W., and Shen, S. *Journal of Polymer Science: Part B: Polym. Phys.* **42**, 2649 (2004).

[16] Madhusudanan, P. M., Krishnan, K., and Ninan, K. N. *Thermochim Acta* **97**, 189 (1986).

[17] Atarsia, A., and Boukhilir, R. *Polym. Eng. Sci.* **40**, 607 (2000).

[18] Vyazovkin, S., Mititelu, A., and Sbirrazzuoli, N. *Macromol. Rapid Commun.* **24**, 1060 (2003).

[19] Rosu, D., Cascaval, C. N., Mustata, F., and Ciobanu, C. *Thermochimica Acta.* **383**, 119 (2002).

[20] Málek, J. *Thermochim. Acta.* **200**, 257 (1992).

[21] Šesták, J., and Berggren, G. *Thermochimica Acta.* **3**, 1 (1971).

[22] Rosu, D., Mititelu, A., and Cascaval, C. N. *Polym. Test.* **23**, 209 (2004).